Prion Protein Devoid of the Octapeptide Repeat Region Delays BSE Pathogenesis in Mice

Hideyuki Hara,[a,*] Hironori Miyata,[b,*] Nandita Rani Das,[a,*] Junji Chida,[a] Tatenobu Yoshimochi,[a,c] Keiji Uchiyama,[a] Hitomi Watanabe,[d] Gen Kondoh,[d] Takashi Yokoyama,[e] Suehiro Sakaguchi[a]#

Division of Molecular Neurobiology, The Institute for Enzyme Research (KOSOKEN), Tokushima University, Kuramoto, Tokushima, Japan[a]; Animal Research Center, School of Medicine, University of Occupational and Environmental Health, Yahatanishi, Kitakyushu, Japan[b]; Student Laboratory, Faculty of Medicine, Tokushima University, Kuramoto, Tokushima, Japan[c]; Laboratory of Integrative Biological Science, Institute for Frontier Life and Medical Sciences, Kyoto University, Kyoto, Japan[d]; National Institute of Animal Health (NIAH), National Agriculture and Food Research Organization (NARO), Tsukuba, Ibaraki, Japan[e].

Running Head: The Role of the OR Region in BSE Pathogenesis

#Address correspondence to Suehiro Sakaguchi, sakaguchi@tokushima-u.ac.jp.

H.H., H.M. and N.D.R. contributed equally to this work.

Word count for the abstract: 232 (Word count for the importance: 126)

Word count for the text: 4,893

ABSTRACT

Conformational conversion of the cellular isoform of prion protein PrP^{C}, into the abnormally folded, amyloidogenic isoform, PrP^{Sc}, is a key pathogenic event in prion diseases including Creutzfeldt-Jakob disease in humans and scrapie and bovine spongiform encephalopathy (BSE) in animals. We previously reported that the octapeptide repeat (OR) region could be dispensable for converting PrP^{C} into PrP^{Sc} after infection with RML prions. We demonstrated that mice transgenically expressing mouse PrP with deletion of the OR region on the PrP-knockout background, designated Tg(PrPΔOR)/*Prnp*$^{0/0}$ mice, did not reduce susceptibility to RML scrapie prions, with abundant accumulation of PrP^{Sc}ΔOR in their brains. We show here that Tg(PrPΔOR)/*Prnp*$^{0/0}$ mice were highly resistant to BSE prions, developing the disease with markedly elongated incubation times after infection with BSE prions. The conversion of PrPΔOR into PrP^{Sc}ΔOR was markedly delayed in their brains. These results suggest that the OR region may have a crucial role in the conversion of PrP^{C} into PrP^{Sc} after infection with BSE prions. However, Tg(PrPΔOR)/*Prnp*$^{0/0}$ mice remained susceptible to RML and 22L scrapie prions, developing the disease without elongated incubation times after infection with RML and 22L prions. PrP^{Sc}ΔOR accumulated only slightly less in the brains of RML- or 22L-infected Tg(PrPΔOR)/*Prnp*$^{0/0}$ mice than PrP^{Sc} in control wild-type mice. Taken together, these results indicate that the OR region of PrP^{C} could play a differential role in the pathogenesis of BSE prions and RML or 22L scrapie prions.

IMPORTANCE

Structure-function relationship studies of PrP^{C} conformational conversion into PrP^{Sc} are worthwhile to understand the mechanism of the conversion of PrP^{C} into PrP^{Sc}. We show here that, by inoculating the three different prion strains RML, 22L and BSE prions, into Tg(PrPΔOR)/$Prnp^{0/0}$ mice, the OR region could play a differential role in the conversion of PrP^{C} into PrP^{Sc} after infection with RML or 22L scrapie prions and BSE prions. PrPΔOR was efficiently converted into PrP^{Sc}ΔOR after infection with RML and 22L prions. However, the conversion of PrPΔOR into PrP^{Sc}ΔOR was markedly delayed after infection with BSE prions. Further investigation into the role of the OR region in the conversion of PrP^{C} into PrP^{Sc} after infection with BSE prions might be helpful for understanding the pathogenesis of BSE prions.

KETWORDS: Prion, Prion protein, Octapeptide repeat, Bovine spongiform encephalopathy (BSE), Scrapie.

INTRODUCTION

Prions are causative agents of prion diseases, a group of fatal neurodegenerative disorders, which include Creutzfeldt-Jakob disease and Gerstmann-Sträussler-Scheinker disease in humans and scrapie and bovine spongiform encephalopathy (BSE) in animals (1). Prions are believed to consist of the abnormally folded, relatively proteinase K (PK)-resistant isoform of prion protein, designated PrP^{Sc}, and propagate through conformational conversion of the PK-sensitive, cellular isoform of PrP, PrP^{C}, into PrP^{Sc} (1). PrP^{C} is a membrane glycoprotein tethered to the cell surface via a glycosylphosphatidylinositol moiety expressed most abundantly in the central nervous system, particularly by neurons (2). We and others have shown that mice devoid of PrP^{C} (*Prnp*$^{0/0}$) are resistant to prions, neither developing the disease nor propagating prions even after intracerebral inoculation with the prions (3-6), clearly indicating that the conversion of PrP^{C} into PrP^{Sc} is a key pathogenic event in prion diseases.

There is the so-called octapeptide repeat (OR) region, which consists of 5 copies of an octapeptide sequence in most mammalian species and 6 copies in a dominant population of cattle, in the N-terminal domain of PrP^{C} (7-10). Insertional mutations of one or more extra octapeptide sequences in the OR region leads to spontaneous conversion of the mutant PrP into the pathogenic PrP. This eventually causes hereditary prion diseases in humans (11). Transgenic mice expressing mouse PrP with an insertion of 9 additional OR sequences (14 OR sequences in total), designated Tg(PG14) mice, or bovine PrP with an insertion of an additional 4 OR sequences (10 OR sequences in total), bo10ORTg mice,

were shown to spontaneously develop neurodegenerative disease with accumulation of the relatively PK-resistant, but non-infectious PrP in their brains (12-14). Thus, insertion of extra octapeptide sequences in the OR region could render the mutant PrP structurally unstable, thereby causing conformational changes in the mutant PrP to form pathogenic PrP.

Insertion of extra octapeptide sequences in the OR region has also been shown to increase susceptibility to BSE prions in mice. Bo10ORTg and bo7ORTg mice were reported to develop prion disease earlier than control bo6ORTg mice after infection with BSE prions (14, 15). Conversely, deletion of one octapeptide sequence in the OR region was reported to reduce susceptibility to BSE prions in mice (16). These results suggest that the OR region could have an important role in the pathogenesis of BSE prions. However, we previously showed that *Prnp*$^{0/0}$ mice transgenic for mouse PrP with deletion of the OR region alone, designated Tg(PrPΔOR)/*Prnp*$^{0/0}$ mice, did not have reduced susceptibility to RML scrapie prions, developing the disease without elongated incubation times after infection with RML prions (17). Taken together, these results suggest that the OR region could have a differential role in the pathogenesis of BSE and RML prions.

In the present study, to verify this possibility, we intracerebrally inoculated Tg(PrPΔOR)/*Prnp*$^{0/0}$ mice with BSE and RML prions. We also inoculated Tg mice with 22L scrapie prions. Tg(PrPΔOR)/*Prnp*$^{0/0}$ mice inoculated with RML and 22L prions developed the disease without elongated incubation times. In contrast, incubation times were markedly elongated in Tg(PrPΔOR)/*Prnp*$^{0/0}$ mice inoculated with BSE prions, with delayed accumulation of PrP^{Sc}ΔOR in their brains. These results clearly show that the OR region

plays a differential role in the pathogenesis of BSE prions and RML or 22L scrapie prions.

RESULTS

Tg(PrPΔOR)/*Prnp*$^{0/0}$ mice are highly resistant to BSE prions, but susceptible to RML and 22L prions

To investigate the role of the OR region in prion pathogenesis, we intracerebrally inoculated Tg(PrPΔOR)/*Prnp*$^{0/0}$ and C57BL/6 WT mice with RML, 22L, and BSE prions. As we previously reported (17), RML-inoculated Tg(PrPΔOR)/*Prnp*$^{0/0}$ mice displayed foreleg paresis in addition to other disease-specific symptoms observed in control WT mice, such as emaciation, ruffled body hair, kyphosis, crossing leg, and paralysis of the hind legs. 22L-inoculated Tg(PrPΔOR)/*Prnp*$^{0/0}$ mice also developed foreleg paresis. Other symptoms were commonly observed in 22L-infected Tg(PrPΔOR)/*Prnp*$^{0/0}$ and WT mice. BSE-infected Tg(PrPΔOR)/*Prnp*$^{0/0}$ and WT mice developed similar symptoms. Consistent with our previous results (17), incubation and survival times were shortened in Tg(PrPΔOR)/*Prnp*$^{0/0}$ mice inoculated with RML prions compared to control WT mice **(Table 1,** $p<0.0001$**)**. WT mice developed the disease at 159 ± 2 (average ± standard deviation) days post-inoculation (dpi) and became terminal at 175 ± 3 dpi while incubation and survival times in Tg(PrPΔOR)/*Prnp*$^{0/0}$ mice were shortened by 29 and 35 days, respectively **(Table 1)**. Tg(PrPΔOR)/*Prnp*$^{0/0}$ mice express PrPΔOR in their brains about 1.7 times more than PrP^{C} in WT mice **(Fig. 1A)**. The higher susceptibility of Tg(PrPΔOR)/*Prnp*$^{0/0}$ mice to RML

prions could be due to higher expression of PrPΔOR in Tg(PrPΔOR)/*Prnp*$^{0/0}$ mice than PrP^{C} in WT mice. Tg(PrPΔOR)/*Prnp*$^{0/0}$ mice also showed higher susceptibility to 22L prions than WT mice. Incubation and survival times were 143 ± 1 and 156 ± 2 dpi in control WT mice, but shortened by 32 and 24 days in Tg(PrPΔOR)/*Prnp*$^{0/0}$ mice inoculated with 22L prions, respectively **(Table 1,** p<0.0001**)**. In contrast, Tg(PrPΔOR)/*Prnp*$^{0/0}$ mice exhibited markedly reduced susceptibility to BSE prions. Incubation and survival times were elongated by 141 and 141 days, respectively, in Tg(PrPΔOR)/*Prnp*$^{0/0}$ mice from 172 ± 6 and 180 ± 8 dpi in WT mice inoculated with BSE prions, respectively **(Table 1,** p<0.0001**)**. These results show that Tg(PrPΔOR)/*Prnp*$^{0/0}$ mice are highly resistant to BSE prions, but remain susceptible to RML and 22L prions, indicating that the OR region could have a crucial role in determination of the susceptibility to BSE prions in mice.

To confirm that the reduced susceptibility to BSE prions in Tg(PrPΔOR)/*Prnp*$^{0/0}$ mice is not a specific phenotype in the Tg line used, we produced another line of Tg(PrPΔOR)/*Prnp*$^{0/0}$ mice, hereafter referred to as Tg(PrPΔOR-3608)/*Prnp*$^{0/0}$. They expressed PrPΔOR in their brains at a similar level to PrP^{C} in *Prnp*$^{+/0}$ mice **(Fig. 1B)**. The expression levels of PrPΔOR in Tg(PrPΔOR-3608)/*Prnp*$^{0/0}$ mice and PrP^{C} in *Prnp*$^{+/0}$ mice are at 45 ± 9 and 51 ± 5% of those of PrP^{C} in WT mice, respectively (p=0.29). We thus intracerebrally inoculated BSE prions into Tg(PrPΔOR-3608)/*Prnp*$^{0/0}$ mice and control *Prnp*$^{+/0}$ mice as controls. Longer incubation times were also observed in Tg(PrPΔOR-3608)/*Prnp*$^{0/0}$ mice after inoculation with BSE prions, compared to control *Prnp*$^{+/0}$ mice **(Table 2,** p<0.0001**)**. *Prnp*$^{+/0}$ mice developed the disease at 274 ± 6 dpi and

145 became terminal at 290 ± 10 dpi while Tg(PrPΔOR-3608)/*Prnp*$^{0/0}$ mice succumbed to the
146 disease at 335 ± 26 dpi, becoming terminal at 343 ± 27 dpi **(Table 2)**. The lower
147 susceptibility of Tg(PrPΔOR-3608)/*Prnp*$^{0/0}$ mice to BSE prions than that of *Prnp*$^{+/0}$ mice
148 despite the similar expression of PrPΔOR in Tg(PrPΔOR-3608)/*Prnp*$^{0/0}$ mice to PrP^{C} in
149 *Prnp*$^{+/0}$ mice reinforces that the OR region could have an important role in determination of
150 the susceptibility to BSE prions.
151
152 **The OR region is not essential for the conversion of PrP^{C} into PrP^{Sc} and brain**
153 **pathologies**
154 To investigate the role of the OR region in the conversion of PrP^{C} into PrP^{Sc}, we
155 investigated the brains of terminally ill Tg(PrPΔOR)/*Prnp*$^{0/0}$ mice infected with RML, 22L,
156 and BSE prions for PrP^{Sc}ΔOR. To detect PrP^{Sc}ΔOR, the brain homogenates were treated
157 with PK and then subjected to Western blotting with 6D11 anti-PrP antibody (Ab), which
158 recognizes residues 93-109 of mouse PrP. Consistent with our previous results (17),
159 PrP^{Sc}ΔOR was detected slightly but significantly less in the brains of RML-infected,
160 terminally ill Tg(PrPΔOR)/*Prnp*$^{0/0}$ mice than PrP^{Sc} in control WT mice **(Fig. 2A,** p=0.006**)**.
161 PrP^{Sc}ΔOR was also detected in the brains of 22L-infected, terminally ill
162 Tg(PrPΔOR)/*Prnp*$^{0/0}$ mice slightly less than PrP^{Sc} in control WT mice **(Fig. 2B,** p=0.136**)**.
163 However, PrP^{Sc}ΔOR was accumulated in the brains of BSE-infected, terminally ill
164 Tg(PrPΔOR)/*Prnp*$^{0/0}$ mice more abundantly than PrP^{Sc} in control WT mice **(Fig. 2C,**
165 p=0.028**)**. Immunohistochemistry revealed indistinguishable staining for PrP^{Sc} and

PrP^{Sc}ΔOR throughout the brain slices of terminally ill WT and Tg(PrPΔOR)/*Prnp*$^{0/0}$ mice infected with RML, 22L, and BSE prions **(Fig. 3A-D)**. These results indicate that, while the OR region is not essential for the conversion of PrP^{C} into PrP^{Sc} after infection with prions, it could affect the final accumulation levels of PrP^{Sc} in brains in a strain-dependent manner.

We also pathologically investigated the brains of RML-, 22L-, and BSE-infected, terminally ill Tg(PrPΔOR)/*Prnp*$^{0/0}$ and WT mice for vaculolation. No significant difference in the number of vacuoles was detected in each brain area between Tg(PrPΔOR)/*Prnp*$^{0/0}$ and WT mice infected with RML, 22L, and BSE prions **(Fig. 4A-D, Fig. 5A-D)**, suggesting that PrP^{Sc}ΔOR and PrP^{Sc} might be similarly pathogenic in brains.

Delayed brain accumulation of PrP^{Sc}ΔOR in BSE-infected Tg(PrPΔOR)/*Prnp*$^{0/0}$ mice

To gain insights into the reduced susceptibility of Tg(PrPΔOR)/*Prnp*$^{0/0}$ mice to BSE prions, we sacrificed WT and Tg(PrPΔOR)/*Prnp*$^{0/0}$ mice at 190 dpi with BSE prions and compared the levels of PrP^{Sc}ΔOR accumulated in the brains of Tg(PrPΔOR)/*Prnp*$^{0/0}$ mice to those of PrP^{Sc} in WT mice. WT mice were terminally ill around 190 dpi. However, Tg(PrPΔOR)/*Prnp*$^{0/0}$ mice were still healthy by 190 dpi. PrP^{Sc}ΔOR was detected at very low levels in Tg(PrPΔOR)/*Prnp*$^{0/0}$ mice, compared to those of PrP^{Sc} in WT mice **(Fig. 6A and B,** p=0.0007**)**. These results indicate that the conversion of PrPΔOR into PrP^{Sc}ΔOR is less efficient than that of full-length PrP^{C} into PrP^{Sc} after infection with BSE prions, suggesting that the OR region could be important for BSE prions to convert PrP^{C} into PrP^{Sc}. It is therefore possible that the reduced susceptibility to BSE prions in Tg(PrPΔOR)/*Prnp*$^{0/0}$

mice could be attributable to the inefficient conversion of PrPΔOR into PrP^{Sc}ΔOR after infection with BSE prions.

The pre-OR region in PrP^{Sc}ΔOR is PK-resistant

We previously showed that the pre-OR region consisting of residues 23-50 of PrP^{Sc}ΔOR produced in the brains of RML-infected Tg(PrPΔOR)/$Prnp^{0/0}$ mice forms a PK-resistant conformation (17). To investigate whether or not 22L and BSE prions could also convert the pre-OR region into a PK-resistant structure upon the conversion of PrPΔOR into PrP^{Sc}ΔOR, we treated 22L- and BSE-infected as well as RML-infected Tg(PrPΔOR)/$Prnp^{0/0}$ brain homogenates with PK. They were then subjected to Western blotting with IBL-N anti-PrP Abs, which were raised against a pre-OR synthetic peptide comprising of residues 24-37 (18). The Abs exhibited no PK-resistant signals in the RML-, 22L-, and BSE-infected WT brain homogenates **(Fig. 7A-C)**. This is consistent with the pre-OR region of full-length PrP^{Sc} being PK-sensitive. However, PK-resistant signals were observed in the RML-, 22L-, and BSE-infected Tg(PrPΔOR)/$Prnp^{0/0}$ brain homogenates **(Fig. 7A-C)**, indicating that the pre-OR region of PrP^{Sc}ΔOR is converted into a PK-resistant structure after infection with RML, 22L, and BSE prions.

Tg(PrPΔOR)/$Prnp^{0/0}$ mice are also highly resistant to secondarily inoculated PrP^{Sc}ΔOR-BSE prions

Differences in the primary sequence between PrP^{C} in recipient animals and PrP^{Sc} in an

inoculum often create the so-called prion transmission barrier leading to elongation of incubation times in recipient animals (19). If a prion transmission barrier is responsible for longer incubation times in primary inoculated mice, secondary inoculation into mice with the same genotype causes shorter incubation times. To investigate whether or not PrPΔOR might create a prion transmission barrier against full-length PrP^{Sc} and thereby render Tg(PrPΔOR)/$Prnp^{0/0}$ mice less susceptible to BSE prions, we secondarily inoculated Tg(PrPΔOR)/$Prnp^{0/0}$ and WT mice by the intracerebral route with brain homogenates from BSE-infected, terminally ill Tg(PrPΔOR)/$Prnp^{0/0}$ mice containing PrP^{Sc}ΔOR. We also secondarily inoculated Tg(PrPΔOR)/$Prnp^{0/0}$ and WT mice with brain homogenates from RML- and 22L-infected, terminally ill Tg(PrPΔOR)/$Prnp^{0/0}$ mice. Similar clinical symptoms were observed in Tg(PrPΔOR)/$Prnp^{0/0}$ mice as well as WT mice after primary and secondary inoculation with RML-, 22L-, or BSE-infected Tg(PrPΔOR)/$Prnp^{0/0}$ brain homogenate. Incubation times were slightly but not significantly shorter in Tg(PrPΔOR)/$Prnp^{0/0}$ mice secondarily inoculated with RML-infected Tg(PrPΔOR)/$Prnp^{0/0}$ brain homogenates, compared to control WT mice **(Table 3,** $p>0.3$**)**. 22L-infected Tg(PrPΔOR)/$Prnp^{0/0}$ brain homogenates caused significantly shorter incubation times in Tg(PrPΔOR)/$Prnp^{0/0}$ mice than in WT mice **(Table 3,** $p<0.001$**)**. However, incubation times were still longer in Tg(PrPΔOR)/$Prnp^{0/0}$ mice than in WT mice even after secondary inoculation with the BSE-infected Tg(PrPΔOR)/$Prnp^{0/0}$ brain homogenate **(Table 3)**. WT mice developed the disease at 165 ± 8 dpi whereas Tg(PrPΔOR)/$Prnp^{0/0}$ mice succumbed to the disease with longer incubation times of 307 ± 9 dpi **(Table 3,** $p<0.0001$**)**. These results

indicate that the different primary sequence between PrPΔOR and WT PrP^{Sc} does not create a transmission barrier for BSE prions.

WT mice infected with PrP^{Sc}- and PrP^{Sc}ΔOR-prions accumulate PrP^{Sc} with the same biochemical properties

To assess the pathogenic effects of PrP^{Sc}ΔOR-prions on the conversion of PrP^{C} into PrP^{Sc}, we investigated accumulation levels, the PK-resistant core size, and glycosylation patterns of PrP^{Sc} molecules in the brains of WT mice inoculated with RML-, 22L-, or BSE-infected Tg(PrPΔOR)/*Prnp*$^{0/0}$ and WT brain homogenates containing PrP^{Sc}ΔOR and PrP^{Sc}, respectively. Western blotting with 6D11 anti-PrP Ab revealed similar amounts of PrP^{Sc} accumulated in terminally ill WT mice inoculated with PrP^{Sc} and PrP^{Sc}ΔOR of RML, 22L, or BSE prions **(Fig. 8A)**. Similar migration patterns were also observed for PrP^{Sc} in WT mice inoculated with RML-, 22L-, or BSE-PrP^{Sc} and -PrP^{Sc}ΔOR **(Fig. 8A)**. The deglycosylated, PK-resistant fragment of PrP^{Sc} in these brains also showed the same migration distance **(Fig. 8B)**. These results suggest that the PK cleavage site is the same for PrP^{Sc} produced after inoculation with RML-, 22L-, or BSE-PrP^{Sc} and -PrP^{Sc}ΔOR. We also investigated glycosylation patterns of PrP^{Sc} in these brains. The ratio of di-, mono-, and un-glycosylated forms of PrP^{Sc} in WT mice inoculated with RML-, 22L-, or BSE-PrP^{Sc}ΔOR were similar to those of PrP^{Sc} in WT mice inoculated with RML-, 22L-, or BSE-PrP^{Sc} **(Fig. 8C)**. Taken together, these results indicate that the biochemical properties of PrP^{Sc} produced in WT mice after inoculation with PrP^{Sc}- and PrP^{Sc}ΔOR-prions are similar, suggesting that

250 PrP^{Sc}ΔOR-prions might have the same pathogenic properties as PrP^{Sc}-prions.

251

252 **DISCUSSION**

253 In the present study, we studied the role of the OR region for PrP^{C} to support prion infection
254 by inoculating RML, 22L, and BSE prions into Tg(PrPΔOR)/*Prnp*$^{0/0}$ mice, which express
255 PrP with a deletion of the OR region alone on the *Prnp*$^{0/0}$ background. Compared to control
256 WT mice, Tg(PrPΔOR)/*Prnp*$^{0/0}$ mice had accelerated disease, exhibiting shorter incubation
257 times after infection with RML and 22L prions. Shorter incubation times in RML-inoculated
258 Tg(PrPΔOR)/*Prnp*$^{0/0}$ mice are consistent with our previous results (17). The length of
259 incubation times inversely correlates to the expression levels of PrP^{C} in animals infected
260 with prions (20). Tg(PrPΔOR)/*Prnp*$^{0/0}$ mice express PrPΔOR in their brains more than PrP^{C}
261 in WT mice. Therefore, the higher susceptibility of Tg(PrPΔOR)/*Prnp*$^{0/0}$ mice to RML and
262 22L prions could be due to the higher expression of PrPΔOR in their brains, suggesting that
263 the OR region of PrP^{C} might be dispensable for RML and 22L infection in mice. In contrast,
264 in spite of the higher expression of PrPΔOR, Tg(PrPΔOR)/*Prnp*$^{0/0}$ mice were highly
265 resistant to BSE prions, exhibiting markedly elongated incubation times after infection with
266 BSE prions, indicating that the OR region could play a crucial role for PrP^{C} to support BSE
267 infection in mice.

268 The so-called prion transmission barrier often occurs when PrP^{Sc} in an inoculum
269 and PrP^{C} in recipient animals differ in primary sequence, interfering with prion infection
270 and eventually causing elongated incubation times in the recipient animals (21, 22).

271 However, Tg(PrPΔOR)/*Prnp*$^{0/0}$ mice remained highly resistant to BSE prions, developing
272 the disease with longer incubation times than WT mice, even after secondary inoculation
273 with brain homogenates from BSE-infected, terminally ill Tg(PrPΔOR)/*Prnp*$^{0/0}$ mice, which
274 contain PrP^{Sc}ΔOR. The longer incubation times of Tg(PrPΔOR)/*Prnp*$^{0/0}$ mice secondarily
275 inoculated with PrP^{Sc}ΔOR-associated BSE prions indicate that the reduced susceptibility of
276 Tg(PrPΔOR)/*Prnp*$^{0/0}$ mice to full-length PrP^{Sc}-associated BSE prions primarily inoculated is
277 not due to the different primary sequences between PrP^{Sc} in the inoculum and PrPΔOR in
278 the recipient mice. This reinforces the crucial role of the OR region in BSE infection.
279 Similar strain-dependent different susceptibility has been reported in mice
280 transgenically expressing PrP with specific mutations or deletions in the sequence. *Prnp*$^{0/0}$
281 mice transgenic for mouse PrP with a serine residue at codon 170, designated
282 Tg(PrP-170S)/*Prnp*$^{0/0}$ mice, became highly resistant to RML and 79A prions, but were still
283 susceptible to 22L and ME7 prions (23). Tg(OvPrP-V136)/*Prnp*$^{0/0}$ mice expressing ovine
284 PrP with a valine residue at codon 136 on the *Prnp*$^{0/0}$ background were still susceptible to
285 SSBP1 prions, but became resistant to CH1641 prions (24). We previously reported that
286 Tg(MHM2Δ23-88)/*Prnp*$^{0/0}$ mice, which express mouse-hamster chimeric PrP with the
287 deletion of residues 23-88, became highly resistant to RML, but still susceptible to 22L
288 prions (25). Elucidation of the mechanism for the strain-dependent susceptibility would be
289 important for understanding of the pathogenesis of prion diseases.
290 The conversion efficiency of PrP^{C} into PrP^{Sc} is a key factor determining prion
291 susceptibility. Indeed, the pathogenic PrPs were undetectable or much less accumulated in

292 the brains of Tg(PrP-170S)/*Prnp*$^{0/0}$, Tg(OvPrP-V136)/*Prnp*$^{0/0}$, or Tg(MHM2Δ23-88)/*Prnp*$^{0/0}$
293 mice inoculated with resistant prion strains, but not with susceptible prion strains (23-25).
294 We also showed that PrP^{Sc}ΔOR was accumulated much less in the brains of
295 Tg(PrPΔOR)/*Prnp*$^{0/0}$ mice than PrP^{Sc} in control WT mice at 190 dpi with BSE prions,
296 indicating that, compared to the conversion of PrP^{C} into PrP^{Sc}, the conversion of PrPΔOR
297 into PrP^{Sc}ΔOR is much more inefficient after infection with BSE prions. However, RML- or
298 22L-inoculated Tg(PrPΔOR)/*Prnp*$^{0/0}$ mice accumulated PrP^{Sc}ΔOR in their brains only
299 slightly less than or similarly to PrP^{Sc} in control WT mice, respectively, suggesting that
300 RML and 22L prions could efficiently convert PrPΔOR into PrP^{Sc}ΔOR. The different
301 efficiency of PrPΔOR to convert into PrP^{Sc}ΔOR after infection with BSE prions and RML
302 or 22L prions indicate that the OR region might be differently involved in the conversion of
303 PrP^{C} into PrP^{Sc} after infection with BSE prions and RML or 22L prions. It is thus
304 conceivable that the different role of the OR region in the conversion of PrP^{C} into PrP^{Sc}
305 could underlie the different susceptibility of Tg(PrPΔOR)/*Prnp*$^{0/0}$ mice to BSE prions and
306 RML or 22L prions.

307 The conformational selection model has been proposed as a mechanism to explain
308 the strain-dependent conversion of PrP^{C} into PrP^{Sc}. PrP^{Sc} molecules from different strains
309 are believed to adopt different conformations (21, 22). Indeed, two different prion strains of
310 transmissible mink encephalopathy, HY and DY, have been shown to produce PrP^{Sc} with
311 strain-specific, different PK cleavage sites (26). DY-PrP^{Sc} has a shorter PK-resistant
312 fragment than HY-PrP^{Sc} (27). The different PK cleavage sites of DY-PrP^{Sc} and HY-PrP^{Sc}

313 indicate different protein conformations of both molecules. The PK-resistant fragment of
314 BSE-PrP^{Sc} is shorter than that of RML- and 22L-PrP^{Sc}, indicating that BSE-PrP^{Sc} forms a
315 different conformation from RML- and 22L-PrP^{Sc}. The conformational selection model
316 postulates that inoculated PrP^{Sc} could select host PrP^{C} as a substrate for conversion on the
317 basis of its conformational compatibility with the host PrP^{C}. Conformational incompatibility
318 between inoculated PrP^{Sc} and host PrP^{C} leads to unsuccessful or insufficient conversion of
319 the host PrP^{C} into PrP^{Sc}, and vice versa, thereby inoculating PrP^{Sc} converting host PrP^{C} into
320 PrP^{Sc} in a strain-dependent manner (21, 22). PrPΔOR might adopt a different conformation
321 from WT PrP^{C}, and the adopted conformation of PrPΔOR might be still compatible with
322 RML- and 22L-PrP^{Sc}, but not with BSE-PrP^{Sc}, therefore PrPΔOR being insufficiently
323 converted into PrP^{Sc}ΔOR. Structural studies have shown that the N-terminal domain of PrP,
324 including the OR region, transiently interacts with the C-terminal globular domain,
325 suggesting that the transient interaction might confer structural stability within the
326 C-terminal globular domain (28, 29). Lack of the OR region might render the C-terminal
327 globular domain of PrPΔOR structurally unstable, thereby reducing the conformational
328 compatibility of PrPΔOR with BSE-PrP^{Sc}, but not with RML- and 22L-PrP^{Sc}. Alternatively,
329 since the OR region binds Cu^{2+} ions via histidine residues (30), lack of Cu^{2+} ions might
330 cause conformational incompatibility of PrPΔOR with BSE-PrP^{Sc}.
331 Other mechanisms might also be possible. Upon the conversion of PrP^{C} into PrP^{Sc},
332 the OR region undergoes conformational changes to form a trypsin-resistant structure (31).
333 It is thus possible that the conformational changes of the OR region might be important for

334 BSE prions to convert PrP^{C} into PrP^{Sc}, therefore lack of the OR region reduces the
335 conversion of PrP^{C} into PrP^{Sc} after infection with BSE prions. The N-terminal domain of
336 PrP^{C}, including the OR region, is highly flexible and displays a marked conformational
337 heterogeneity (29, 32, 33). Therefore, it is also possible that lack of the OR region might
338 reduce the N-terminal conformational heterogeneity in PrPΔOR, rendering PrPΔOR
339 resistant to BSE prions, but not to RML and 22L prions. The conversion of PrP^{C} into PrP^{Sc}
340 has been suggested to take place on the cell surface and/or along the endocytic pathway to
341 lysosomes (34, 35). The OR region has been shown to be important for internalization of
342 PrP^{C} (36). Defective internalization of PrPΔOR might disturb conversion into PrP^{Sc}ΔOR,
343 specifically after infection with BSE prions. Further studies are needed to elucidate the
344 mechanism of the strain-specific conversion of PrP^{C} into PrP^{Sc}. Elucidation of the exact role
345 of the OR region in the conversion of PrP^{C} into PrP^{Sc} after infection with BSE prions might
346 be helpful for understanding strain-specific conversion of PrP^{C} into PrP^{Sc}.

347 At terminal stages, PrP^{Sc}ΔOR was higher in the brains of BSE-infected
348 Tg(PrPΔOR)/$Prnp^{0/0}$ mice than PrP^{Sc} in control WT mice. However, PrP^{Sc}ΔOR was
349 accumulated slightly less or similarly in the brains of RML- or 22L-infected, terminally ill
350 Tg(PrPΔOR)/$Prnp^{0/0}$ mice, respectively, compared to PrP^{Sc} in control WT mice. This is
351 consistent with our previous results that PrP^{Sc}ΔOR was slightly lower in the brains of
352 Tg(PrPΔOR)/$Prnp^{0/0}$ mice than WT mice after infection with RML prions (17).
353 Tg(PrPΔOR)/$Prnp^{0/0}$ mice developed the disease earlier than WT mice after infection with
354 RML and 22L prions whereas they succumbed to the disease much later than WT mice after

infection with BSE prions. Therefore, the different incubation times might affect the final levels of PrP^{Sc}ΔOR in the brains of Tg(PrPΔOR)/*Prnp*$^{0/0}$ mice infected with RML, 22L and BSE prions.

The pre-OR region was converted into a PK-resistant structure upon the conversion of PrPΔOR into PrP^{Sc}ΔOR, but not upon the conversion of full-length PrP^{C} into PrP^{Sc}. We showed that PrP^{Sc}- and PrP^{Sc}ΔOR-associated BSE prions were highly pathogenic in WT mice but poorly so in Tg(PrPΔOR)/*Prnp*$^{0/0}$ mice. We also showed that PrP^{Sc}ΔOR could have similar pathogenic properties to full-length PrP^{Sc}. Similar amounts of PrP^{Sc}, with the same PK-resistant core size and the same glycosylation patterns, were detected between the brains of terminally ill WT mice inoculated with PrP^{Sc}- and PrP^{Sc}ΔOR-associated prions. These results suggest that the PK-resistant pre-OR region might not affect the pathogenic properties of prions.

We showed that the OR region could be differentially involved in the conversion of PrP^{C} into PrP^{Sc} after infection with BSE prions and RML or 22L prions, suggesting that PrP^{C} might be converted into PrP^{Sc} through an OR region-dependent or -independent mechanism in a strain-dependent way. The major PK cleavage site in PrP^{Sc} is usually located either within the C-terminal part of the OR region or in the region C-terminal to the OR region (37). BSE-PrP^{Sc} has a PK cleavage site outside of the OR region (37), therefore producing a shorter C-terminal fragment after PK treatment. In contrast, RML- and 22L-PrP^{Sc}s have a longer PK-resistant fragment, indicating that the PK cleavage site of RML- and 22L-PrP^{Sc}s is within the OR region. It is thus interesting to speculate that PrP^{Sc}

carrying a PK cleavage site outside of the OR region, like BSE-PrP^{Sc}, might convert PrP^{C} into PrP^{Sc} through the OR region-dependent mechanism. In contrast, PrP^{Sc} with a PK cleavage site within the OR region might convert PrP^{C} into PrP^{Sc} in the OR region-independent way. Investigation of other prions for the relationship between the role of the OR region in the conversion of PrP^{C} into PrP^{Sc} and location of the PK cleavage site in the corresponding PrP^{Sc}s might be worthwhile for further understanding the mechanism for conversion of PrP^{C} into PrP^{Sc}.

MATERIALS AND METHODS

Ethics statements

The Ethics Committees of Animal Care and Experimentation of the University of Occupational and Environmental Health and Tokushima University approved this study (approval number AE08-013, T28-100). Animals were cared for in accordance with The Guiding Principle for Animal Care and Experimentation of the University of Occupational and Environmental Health and Tokushima University and with Japanese Law for Animal Welfare and Care.

Antibodies

The antibodies used in this study are as follow: 6D11 mouse anti-PrP Ab (SIG-399810, BioLegend, San Diego, USA), IBL-N rabbit anti-PrP Ab (18635, Immuno-Biological

Laboratories, Gunma, Japan), mouse anti-ß-actin Ab (A5441, Sigma-Aldrich, St. Louis, USA), anti-mouse IgG, HRP-linked Ab (NA931, GE Healthcare, Little Chalfont, England), and anti-rabbit IgG, HRP-linked Ab (NA934, GE Healthcare).

Animals

Tg(PrPΔOR)/*Prnp*$^{0/0}$ mice with the C57BL/6 background were produced elsewhere (18). In brief, a transgene construct encoding PrPΔOR was injected into the zygotes of C57BL/6 mice to generate Tg(PrPΔOR) mice as described elsewhere (38, 39). The resulting Tg(PrPΔOR) mice were successively mated with Zrch I *Prnp*$^{0/0}$ mice, which had been backcrossed with C57BL/6 mice at least 9 times, to produce the line of Tg(PrPΔOR)/*Prnp*$^{0/0}$ mice. A new line of Tg(PrPΔOR)/*Prnp*$^{0/0}$ mice, designated Tg(PrPΔOR-3608)/*Prnp*$^{0/0}$ mic, were similarly produced in this study. *Prnp*$^{+/0}$ mice were produced by mating of Zrch I *Prnp*$^{0/0}$ mice with C57BL/6 mice. C57BL/6 mice were purchased from Charles River Laboratories Japan (Kanagawa, Japan). CD-1 mice were purchased from Japan SLC Inc. (Shizuoka, Japan).

Prion inoculation

BSE prions originate from the classical type of BSE and have been maintained in CD-1 WT mice by successive intracerebral inoculations (37). RML and 22L prions are passaged in C57BL/6 WT mice. Brains were removed from terminally ill mice infected with RML, 22L, or BSE prions. A single brain was homogenized (10%, w/v) in phosphate-buffered saline

418 (PBS, 11482-15, Nakalai tesque, Osaka, Japan) using Multi-beads shocker (Yasui Kikai,
419 Osaka, Japan) and then diluted 1% with PBS. Two brain homogenates from RML, 22L, or
420 BSE-infected mice were mixed in equal amounts to prepare a brain homogenate inoculum
421 and the resulting inoculum was intracerebrally inoculated into 5-6 week-old C57BL/6 WT,
422 *Prnp*$^{+/0}$, or Tg(PrPΔOR)/*Prnp*$^{0/0}$ mice with a 20 μl-aliquot. Mice were diagnosed as sick
423 when they developed more than five of the following features: emaciation, decreased
424 locomotion, ruffled body hair, ataxic gait, kyphosis, priapism, upright tail, crossing leg, hind
425 leg paresis, and foreleg paresis. Mice were also diagnosed as terminal when they became
426 akinetic.
427
428 **Protease K and PNGase F treatment**
429 Brain homogenates (10%, w/v) were prepared in lysis buffer (50 mM Tris-HCl, pH 7.4,
430 containing 0.5% Triton X-100, 0.5% sodium deoxycholate, and 150 mM NaCl) using
431 Multi-beads shocker (Yasui Kikai). Protein concentration was determined by a
432 bicinchoninic acid (BCA) protein assay kit (23225, Pierce, Rockford, USA) using bovine
433 serum albumin (23209, Pierce) as a standard, and the homogenates were adjusted to 5 mg of
434 protein/ml with the lysis buffer. For sample preparation for analysis of PrP^{Sc}, aliquots of 100
435 μl of the lysates were digested with 10 μg proteinase K (165-21043, PK, Wako Pure
436 Chemical Industries, Osaka, Japan) at 37˚C for 30 min. Peptide N-glycosidase F (P0704L,
437 PNGase F, New England Biolabs, Beverly, USA) was used according to the manufacturer's
438 protocol. In brief, total proteins were denatured in Glycoprotein Denaturing Buffer (B1704S,

New England Biolabs, Beverly, USA) by heating at 100˚C for 10 min and incubated with PNGase F (New England Biolabs) in a reaction buffer containing GlycoBuffer 2 (B3704S, New England Biolabs) and 1% NP-40 (B2704S, New England Biolabs) at 37˚C for 1 h. The samples were finally mixed with sodium dodecyl sulfate (SDS) sample buffer (62.5 mM Tris-HCl pH6.8, containing 5% SDS, 4% β-mercaptoethanol, 5% Glycerol, 0.04% bromophenol blue, and 3 mM EDTA) and heated at 95˚C for 10 min before being subjected to Western blotting.

Western blotting

Proteins were resolved by SDS-polyacrylamide gel electrophoresis and electrically transferred to an Immobilon-P PVDF membrane (IPVH00010, Millipore, Billerica, USA). After blocking with 1% non-fat dry milk in TBST (10 mM Tris-HCl, pH7.4, containing 0.05% Tween-20, and 150 mM NaCl) at room temperature (RT) for 1 h, the membranes were washed 3 times with TBST at RT for 5 min and incubated with the first Ab at 4˚C overnight in TBST containing 0.5% non-fat dry milk. The membranes were then washed 3 times with TBST at RT for 5 min, and incubated with horseradish peroxidase-conjugated secondary Ab at RT for 2h in TBST containing 0.5% non-fat dry milk. After washing 3 times with TBST at RT for 5 min, immunoreactive proteins were visualized using Immobilon Western Chemiluminescent HRP substrate (WBKLS0500, Millipore) and detected by LAS-4000 mini chemiluminescence imaging system (Fuji Film, Tokyo, Japan). Signal intensities were determined by Image Gauge software (Fuji Film).

Hematoxylin-Eosin staining

Paraffin-embedded samples were sectioned at 5 μm. The sectioned samples were deparaffinized, rehydrated, and stained with Mayer's hematoxylin solution (131-09665, Wako Pure Chemical Industries) and 1% Eosin Y solution (051-06515, Wako Pure Chemical Industries). After washing, the samples were mounted with Softmount (192-16301, Wako Pure Chemical Industries).

Immunohistochemistry

Paraffin-embedded samples were sectioned at 5 μm. After deparaffinized, and rehydrated, the samples were autoclaved in 1 mM HCl at 121˚C for 5 min and subsequently washed with PBS. The samples were digested with 50 μg/mL PK in PBS at 37˚C for 30 min, treated with 3 M guanidine thiocyanate at RT for 10 min and then washed with PBS. After blocking with 5% FBS in PBS at RT for 1 h, the samples were incubated with 6D11 anti-PrP Ab at RT for 2 h and washed with PBS. The samples were then treated with ImmPRESS REAGENT Anti-Mouse IgG (MP-7402, Vector Laboratories, Burlingame, USA) at RT for 1 h. After washing with PBS, the samples were incubated with ImmPACT DAB Peroxidase Substrate (SK-4105, Vector Laboratories) for 180 sec for staining.

Statistical analysis

Survival and incubation times were analyzed using the Log-rank(Mantel-Cox) test. Other

data were analyzed using the Student's *t*-test.

ACKNOWLEDGEMENT

We thank Dr. Stanley B. Prusiner for providing Zrch I *Prnp*$^{0/0}$ mice.

FUNDING INFORMATION

This work was supported in part by JSPS KAKENHI 26293212, MEXT KAKENHI 15H01560 and 17H05701, and the Practical Research Project for Rare/Intractable Diseases of the Japan Agency for Medical Research and Development (AMED) to SS and by JSPS KAKENHI 25870479 to HH.

REFERENCES

1. **Prusiner SB.** 1998. Prions. Proc Natl Acad Sci U S A **95**:13363-83.
2. **Stahl N, Borchelt DR, Hsiao K, Prusiner SB.** 1987. Scrapie prion protein contains a phosphatidylinositol glycolipid. Cell **51**:229-40.
3. **Bueler H, Aguzzi A, Sailer A, Greiner RA, Autenried P, Aguet M, Weissmann C.** 1993. Mice devoid of PrP are resistant to scrapie. Cell **73**:1339-47.
4. **Prusiner SB, Groth D, Serban A, Koehler R, Foster D, Torchia M, Burton D,**

Yang SL, DeArmond SJ. 1993. Ablation of the prion protein (PrP) gene in mice prevents scrapie and facilitates production of anti-PrP antibodies. Proc Natl Acad Sci U S A **90**:10608-12.

5. **Manson JC, Clarke AR, McBride PA, McConnell I, Hope J.** 1994. PrP gene dosage determines the timing but not the final intensity or distribution of lesions in scrapie pathology. Neurodegeneration **3**:331-40.

6. **Sakaguchi S, Katamine S, Shigematsu K, Nakatani A, Moriuchi R, Nishida N, Kurokawa K, Nakaoke R, Sato H, Jishage K, Kuno J, Noda T, Miyamoto T.** 1995. Accumulation of proteinase K-resistant prion protein (PrP) is restricted by the expression level of normal PrP in mice inoculated with a mouse-adapted strain of the Creutzfeldt-Jakob disease agent. J Virol **69**:7586-92.

7. **Goldmann W, Hunter N, Martin T, Dawson M, Hope J.** 1991. Different forms of the bovine PrP gene have five or six copies of a short, G-C-rich element within the protein-coding exon. J Gen Virol **72 (Pt 1)**:201-4.

8. **Neibergs HL, Ryan AM, Womack JE, Spooner RL, Williams JL.** 1994. Polymorphism analysis of the prion gene in BSE-affected and unaffected cattle. Anim Genet **25**:313-7.

9. **Ferguson NM, Donnelly CA, Woolhouse ME, Anderson RM.** 1997. A genetic interpretation of heightened risk of BSE in offspring of affected dams. Proc Biol Sci **264**:1445-55.

10. **Schlapfer I, Saitbekova N, Gaillard C, Dolf G.** 1999. A new allelic variant in the

bovine prion protein gene (PRNP) coding region. Anim Genet **30**:386-7.

11. **Prusiner SB.** 1993. Genetic and infectious prion diseases. Arch Neurol **50**:1129-53.

12. **Chiesa R, Piccardo P, Ghetti B, Harris DA.** 1998. Neurological illness in transgenic mice expressing a prion protein with an insertional mutation. Neuron **21**:1339-51.

13. **Chiesa R, Piccardo P, Quaglio E, Drisaldi B, Si-Hoe SL, Takao M, Ghetti B, Harris DA.** 2003. Molecular distinction between pathogenic and infectious properties of the prion protein. J Virol **77**:7611-22.

14. **Castilla J, Gutierrez-Adan A, Brun A, Pintado B, Salguero FJ, Parra B, Segundo FD, Ramirez MA, Rabano A, Cano MJ, Torres JM.** 2005. Transgenic mice expressing bovine PrP with a four extra repeat octapeptide insert mutation show a spontaneous, non-transmissible, neurodegenerative disease and an expedited course of BSE infection. FEBS Lett **579**:6237-46.

15. **Castilla J, Gutierrez-Adan A, Brun A, Pintado B, Parra B, Ramirez MA, Salguero FJ, Diaz San Segundo F, Rabano A, Cano MJ, Torres JM.** 2004. Different behavior toward bovine spongiform encephalopathy infection of bovine prion protein transgenic mice with one extra repeat octapeptide insert mutation. J Neurosci **24**:2156-64.

16. **Brun A, Gutierrez-Adan A, Castilla J, Pintado B, Diaz-San Segundo F, Cano MJ, Alamillo E, Espinosa JC, Torres JM.** 2007. Reduced susceptibility to bovine spongiform encephalopathy prions in transgenic mice expressing a bovine PrP with

five octapeptide repeats. J Gen Virol **88**:1842-9.

17. **Yamaguchi Y, Miyata H, Uchiyama K, Ootsuyama A, Inubushi S, Mori T, Muramatsu N, Katamine S, Sakaguchi S.** 2012. Biological and biochemical characterization of mice expressing prion protein devoid of the octapeptide repeat region after infection with prions. PLoS ONE **7**:e43540.

18. **Yoshikawa D, Yamaguchi N, Ishibashi D, Yamanaka H, Okimura N, Yamaguchi Y, Mori T, Miyata H, Shigematsu K, Katamine S, Sakaguchi S.** 2008. Dominant-negative effects of the N-terminal half of prion protein on neurotoxicity of prion protein-like protein/doppel in mice. J Biol Chem **283**:24202-11.

19. **Scott M, Foster D, Mirenda C, Serban D, Coufal F, Walchli M, Torchia M, Groth D, Carlson G, DeArmond SJ, Westaway D, Prusiner SB.** 1989. Transgenic mice expressing hamster prion protein produce species-specific scrapie infectivity and amyloid plaques. Cell **59**:847-57.

20. **Fischer M, Rulicke T, Raeber A, Sailer A, Moser M, Oesch B, Brandner S, Aguzzi A, Weissmann C.** 1996. Prion protein (PrP) with amino-proximal deletions restoring susceptibility of PrP knockout mice to scrapie. Embo J **15**:1255-64.

21. **Collinge J, Clarke AR.** 2007. A general model of prion strains and their pathogenicity. Science **318**:930-6.

22. **Wadsworth JD, Asante EA, Collinge J.** 2010. Review: contribution of transgenic models to understanding human prion disease. Neuropathology and applied neurobiology **36**:576-97.

565 23. **Striebel JF, Race B, Meade-White KD, LaCasse R, Chesebro B.** 2011. Strain
566 specific resistance to murine scrapie associated with a naturally occurring human
567 prion protein polymorphism at residue 171. PLoS pathogens **7**:e1002275.
568 24. **Saijo E, Kang HE, Bian J, Bowling KG, Browning S, Kim S, Hunter N, Telling**
569 **GC.** 2013. Epigenetic dominance of prion conformers. PLoS pathogens **9**:e1003692.
570 25. **Uchiyama K, Miyata H, Yano M, Yamaguchi Y, Imamura M, Muramatsu N,**
571 **Das NR, Chida J, Hara H, Sakaguchi S.** 2014. Mouse-hamster chimeric prion
572 protein (PrP) devoid of N-terminal residues 23-88 restores susceptibility to 22L
573 prions, but not to RML prions in PrP-knockout mice. PLoS ONE **9**:e109737.
574 26. **Bessen RA, Marsh RF.** 1992. Biochemical and physical properties of the prion
575 protein from two strains of the transmissible mink encephalopathy agent. J Virol
576 **66**:2096-101.
577 27. **Bessen RA, Marsh RF.** 1994. Distinct PrP properties suggest the molecular basis of
578 strain variation in transmissible mink encephalopathy. J Virol **68**:7859-68.
579 28. **James TL, Liu H, Ulyanov NB, Farr-Jones S, Zhang H, Donne DG, Kaneko K,**
580 **Groth D, Mehlhorn I, Prusiner SB, Cohen FE.** 1997. Solution structure of a
581 142-residue recombinant prion protein corresponding to the infectious fragment of
582 the scrapie isoform. Proc Natl Acad Sci U S A **94**:10086-91.
583 29. **Donne DG, Viles JH, Groth D, Mehlhorn I, James TL, Cohen FE, Prusiner SB,**
584 **Wright PE, Dyson HJ.** 1997. Structure of the recombinant full-length hamster
585 prion protein PrP(29-231): the N terminus is highly flexible. Proc Natl Acad Sci U S

A **94**:13452-7.

30. **Brown DR, Qin K, Herms JW, Madlung A, Manson J, Strome R, Fraser PE, Kruck T, von Bohlen A, Schulz-Schaeffer W, Giese A, Westaway D, Kretzschmar H.** 1997. The cellular prion protein binds copper in vivo. Nature **390**:684-7.

31. **Yam AY, Gao CM, Wang X, Wu P, Peretz D.** 2010. The octarepeat region of the prion protein is conformationally altered in PrP(Sc). PloS one **5**:e9316.

32. **Riek R, Hornemann S, Wider G, Glockshuber R, Wuthrich K.** 1997. NMR characterization of the full-length recombinant murine prion protein, mPrP(23-231). FEBS letters **413**:282-8.

33. **Peretz D, Williamson RA, Matsunaga Y, Serban H, Pinilla C, Bastidas RB, Rozenshteyn R, James TL, Houghten RA, Cohen FE, Prusiner SB, Burton DR.** 1997. A conformational transition at the N terminus of the prion protein features in formation of the scrapie isoform. J Mol Biol **273**:614-22.

34. **Borchelt DR, Taraboulos A, Prusiner SB.** 1992. Evidence for synthesis of scrapie prion proteins in the endocytic pathway. J Biol Chem **267**:16188-99.

35. **Goold R, Rabbanian S, Sutton L, Andre R, Arora P, Moonga J, Clarke AR, Schiavo G, Jat P, Collinge J, Tabrizi SJ.** 2011. Rapid cell-surface prion protein conversion revealed using a novel cell system. Nature communications **2**:281.

36. **Taylor DR, Watt NT, Perera WS, Hooper NM.** 2005. Assigning functions to distinct regions of the N-terminus of the prion protein that are involved in its

copper-stimulated, clathrin-dependent endocytosis. J Cell Sci **118**:5141-53.

37. **Hayashi HK, Yokoyama T, Takata M, Iwamaru Y, Imamura M, Ushiki YK, Shinagawa M.** 2005. The N-terminal cleavage site of PrPSc from BSE differs from that of PrPSc from scrapie. Biochem Biophys Res Commun **328**:1024-7.

38. **Brinster RL, Chen HY, Trumbauer ME, Yagle MK, Palmiter RD.** 1985. Factors affecting the efficiency of introducing foreign DNA into mice by microinjecting eggs. Proc Natl Acad Sci U S A **82**:4438-42.

39. **Wilmut I, Hooper ML, Simons JP.** 1991. Genetic manipulation of mammals and its application in reproductive biology. J Reprod Fertil **92**:245-79.

Figure legends

FIG 1. PrPΔOR expression in the brains of Tg(PrPΔOR)/*Prnp*$^{0/0}$ and Tg(PrPΔOR-3608)/*Prnp*$^{0/0}$ mice. (A) Left panel: Western blotting with 6D11 anti-PrP Ab of the brains of WT (n=3), Tg(PrPΔOR)/*Prnp*$^{0/0}$ (n=3), and *Prnp*$^{0/0}$ mice (n=3). Right panel: Expression levels of PrPΔOR in Tg(PrPΔOR)/*Prnp*$^{0/0}$ mice to PrP^{C} in WT mice. (B) Left panel: Western blotting of the brains of WT (n=3), *Prnp*$^{+/0}$ (n=3), Tg(PrPΔOR-3608)/*Prnp*$^{0/0}$ (n=3), and *Prnp*$^{0/0}$ mice (n=3) with 6D11 anti-PrP Ab. Right panel. Expression levels of PrP^{C} in *Prnp*$^{+/0}$ mice and PrPΔOR in Tg(PrPΔOR-3608)/*Prnp*$^{0/0}$ mice compared to PrP^{C} in WT mice. AU, arbitrary unit.

FIG 2. Different levels of PrP^{Sc}ΔOR accumulated in the brains of Tg(PrPΔOR)/*Prnp*$^{0/0}$ mice infected with RML, 22L, and BSE prions at terminal stages. Western blotting with 6D11 anti-PrP Ab of the brains of terminally ill WT (n=3) and Tg(PrPΔOR)/*Prnp*$^{0/0}$ mice (n=3) infected with RML (A), 22L (B), and BSE prions (C) after treatment with (+) or without (-) PK. Right panel, levels of PrP^{Sc}ΔOR in Tg(PrPΔOR)/*Prnp*$^{0/0}$ mice to PrP^{Sc} in WT mice. AU, arbitrary unit. ns, not significant, *, $p<0.05$; **, $p<0.01$.

FIG 3. Indistinguishable distribution of PrP^{Sc} and PrP^{Sc}ΔOR accumulated in the brains of terminally ill WT and Tg(PrPΔOR)/*Prnp*$^{0/0}$ mice. Brain slices from uninfected (A) and RML- (B), 22L- (C), and BSE-infected (D) terminally ill WT (n=3 in each mouse group) and Tg(PrPΔOR)/*Prnp*$^{0/0}$ mice (n=3 in each mouse group) were immunohistochemically stained

639 for PrP^{Sc} and $PrP^{Sc}\Delta OR$ by 6D11 anti-PrP Ab using the HCl-autoclaving method. Three
640 sections from each mouse brain were subjected to investigation of PrP^{Sc} and $PrP^{Sc}\Delta OR$
641 distribution. Cx, Cerebral cortex; Hp, Hippocampus; Th, Thalamus; Cb, Cerebellum. Bar,
642 100 μm.
643
644 FIG 4. Similar vacuolation in the brains of terminally ill WT and Tg(PrPΔOR)/*Prnp*$^{0/0}$ mice.
645 Brain slices from uninfected (A) and RML- (B), 22L- (C), and BSE-infected (D) terminally
646 ill WT (n=3 in each mouse group) and Tg(PrPΔOR)/*Prnp*$^{0/0}$ mice (n=3 in each mouse group)
647 were subjected to HE staining and vacuoles in 0.1 mm^2 areas were counted in various brain
648 regions, including the cerebral cortex, hippocampus, thalamus, and cerebellum, respectively.
649 Three sections from each mouse brain were subjected to the counting of vacuoles.
650
651 FIG 5. Similar pathologies in the brains of terminally ill WT and Tg(PrPΔOR)/*Prnp*$^{0/0}$ mice
652 infected with RML, 22L, or BSE prions. Brain slices from uninfected (A) and RML- (B),
653 22L- (C), and BSE-infected (D) terminally ill WT (n=3 in each mouse group) and
654 Tg(PrPΔOR)/*Prnp*$^{0/0}$ mice (n=3 in each mouse group) were subjected to HE staining. Three
655 sections from each mouse brain were used for the pathological examinations. Cx, Cerebral
656 cortex; Hp, Hippocampus; Th, Thalamus; Cb, Cerebellum. Bar, 100 μm.
657
658 FIG 6. Delayed accumulation of $PrP^{Sc}\Delta OR$ in the brains of Tg(PrPΔOR)/*Prnp*$^{0/0}$ mice
659 infected with BSE prions. (A) Brain homogenates from WT (n=3) and Tg(PrPΔOR)/*Prnp*$^{0/0}$

660 mice (n=3) sacrificed at 190 dpi with BSE prions were treated with (+) or without (-) PK and
661 then subjected to Western blotting with 6D11 anti-PrP Ab. (B) PrP^{Sc} and $PrP^{Sc}\Delta OR$ levels in
662 the lower panels of (A). AU, arbitrary unit. ***, $p<0.001$.
663
664 FIG 7. The pre-OR region of $PrP^{Sc}\Delta OR$ is PK-resistant, but not in WT PrP^{Sc}. Brain
665 homogenates from terminally ill WT (n=3) and Tg(PrPΔOR)/$Prnp^{0/0}$ mice (n=3) infected
666 with RML (A), 22L (B), and BSE prions (C) were treated with (+) or without (-) PK and then
667 subjected to Western blotting with IBL-N anti-PrP Abs.
668
669 FIG 8. Biochemical characterization of PrP^{Sc} produced in WT mice after inoculation with
670 full-length PrP^{Sc}- and $PrP^{Sc}\Delta OR$-prions. (A) Western blotting with 6D11 anti-PrP Ab of the
671 brains of terminally ill WT mice inoculated with RML-, 22L-, or BSE-infected WT and
672 Tg(PrPΔOR)/$Prnp^{0/0}$ brain homogenates. (B) Western blotting with 6D11 anti-PrP Ab of the
673 brains of terminally ill WT mice inoculated with RML-, 22L-, or BSE-infected WT and
674 Tg(PrPΔOR)/$Prnp^{0/0}$ brain homogenates after treatment with PNGase F. (C) Percentage of
675 the di-glycosylated, mono-glycosylated, and un-glycosylated forms of PrP^{Sc} in the brains of
676 terminally ill WT mice inoculated with RML-, 22L-, or BSE-infected WT and
677 Tg(PrPΔOR)/$Prnp^{0/0}$ brain homogenates.

Table 1. Incubation and survival times of WT and Tg(PrPΔOR)/*Prnp*$^{0/0}$ mice inoculated with various prions.

Prions	Recipient mouse	Expression level of PrP[1] (fold)	Diseased mice /Total mice	Incubation times[2] (average ± standard deviation, days)	Survival times[3] (average ± standard deviation, days)	P value[4] [Log-rank(Mantel-Cox) Test]
RML	WT	1	18/18	159 ± 2	175 ± 3	<0.0001
	Tg(PrPΔOR)/*Prnp*$^{0/0}$	1.7	15/15	130 ± 7	140 ± 9	
22L	WT	1	13/13	143 ± 1	156 ± 2	<0.0001
	Tg(PrPΔOR)/*Prnp*$^{0/0}$	1.7	16/16	111 ± 9	132 ± 14	
BSE	WT	1	11/11	172 ± 6	180 ± 8	<0.0001
	Tg(PrPΔOR)/*Prnp*$^{0/0}$	1.7	21/21	313 ± 4	321 ± 4	

[1]Expression levels were compared to those of PrP^{C} in WT mice using Western blotting (ref).

[2]Times to the onset of disease.

[3]Times to the terminal stage of disease.

[4] P values indicate significance of incubation and survival times between WT and Tg(PrPΔOR)/*Prnp*$^{0/0}$ mice.

Table 2. Incubation and survival times of *Prnp*$^{+/0}$ and Tg(PrPΔOR-3608)/*Prnp*$^{0/0}$ mice inoculated with BSE prions.

Prions	Recipient mouse	Expression level of PrP[1] (fold)	Diseased mice /Total mice	Incubation times[2] (average ± standard deviation, days)	Survival times[3] (average ± standard deviation, days)	P value[4] [Log-rank(Mantel-Cox) Test]
BSE	*Prnp*$^{+/0}$	0.5	13/13	274 ± 6	290 ± 10	<0.0001
	Tg(PrPΔOR-3608)/*Prnp*$^{0/0}$	0.5	12/12	335 ± 26	343 ± 27	

[1]Expression levels were compared to those of PrP^{C} in WT mice using Western blotting (ref).

[2]Times to the onset of disease.

[3]Times to the terminal stage of disease.

[4] P value indicates significance of incubation and survival times between Tg(PrPΔOR)/*Prnp*$^{0/0}$ and *Prnp*$^{+/0}$ mice.

Table 3. Tg(PrPΔOR)/*Prnp*$^{0/0}$ mice are still susceptible to RML and 22L prions, but highly resistant to BSE prions, even after secondary inoculation with RML, 22L, and BSE-infected Tg(PrPΔOR)/*Prnp*$^{0/0}$ brain homogenates.

Tg(PrPΔOR)/*Prnp*$^{0/0}$ brain homogenate inoculum	Recipient mouse	Diseased mice /Total mice	Incubation times[1] (average ± standard deviation, days)	Survival times[2] (average ± standard deviation, days)	P value[3] [Log-rank(Mantel-Cox) Test]
RML	Wild-type	10/10	144 ± 3	176 ± 7	>0.3
	Tg(PrPΔOR)/*Prnp*$^{0/0}$	10/10	145 ± 7	164 ± 15	
22L	Wild-type	10/10	148 ± 6	155 ± 4	<0.0001
	Tg(PrPΔOR)/*Prnp*$^{0/0}$	10/10	104 ± 7	109 ± 3	
BSE	Wild-type	6/6	165 ± 8	179 ± 9	<0.001
	Tg(PrPΔOR)/*Prnp*$^{0/0}$	6/6	307 ± 9	331 ± 20	

[1]Times to the onset of disease.

[2]Times to the terminal stage of disease.

[3]P values indicate significance of incubation and survival times between Tg(PrPΔOR)/*Prnp*$^{0/0}$ and WT mice.

Figure 1

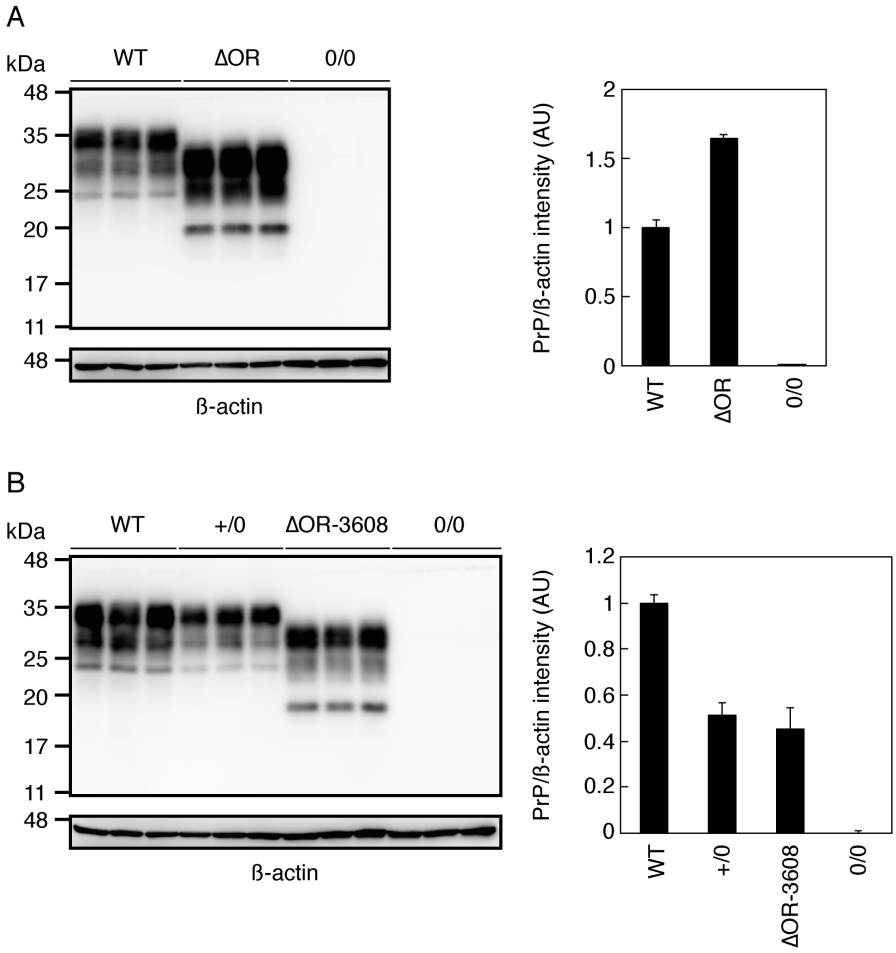
A
kDa
WT
ΔOR
0/0
48
35
25
20
17
11
48
ß-actin
PrP/ß-actin intensity (AU)
2
1.5
1
0.5
0
WT
ΔOR
0/0
B
kDa
WT
+/0
ΔOR-3608
0/0
48
35
25
20
17
11
48
ß-actin
PrP/ß-actin intensity (AU)
1.2
1
0.8
0.6
0.4
0.2
0
WT
+/0
ΔOR-3608
0/0

Figure 2

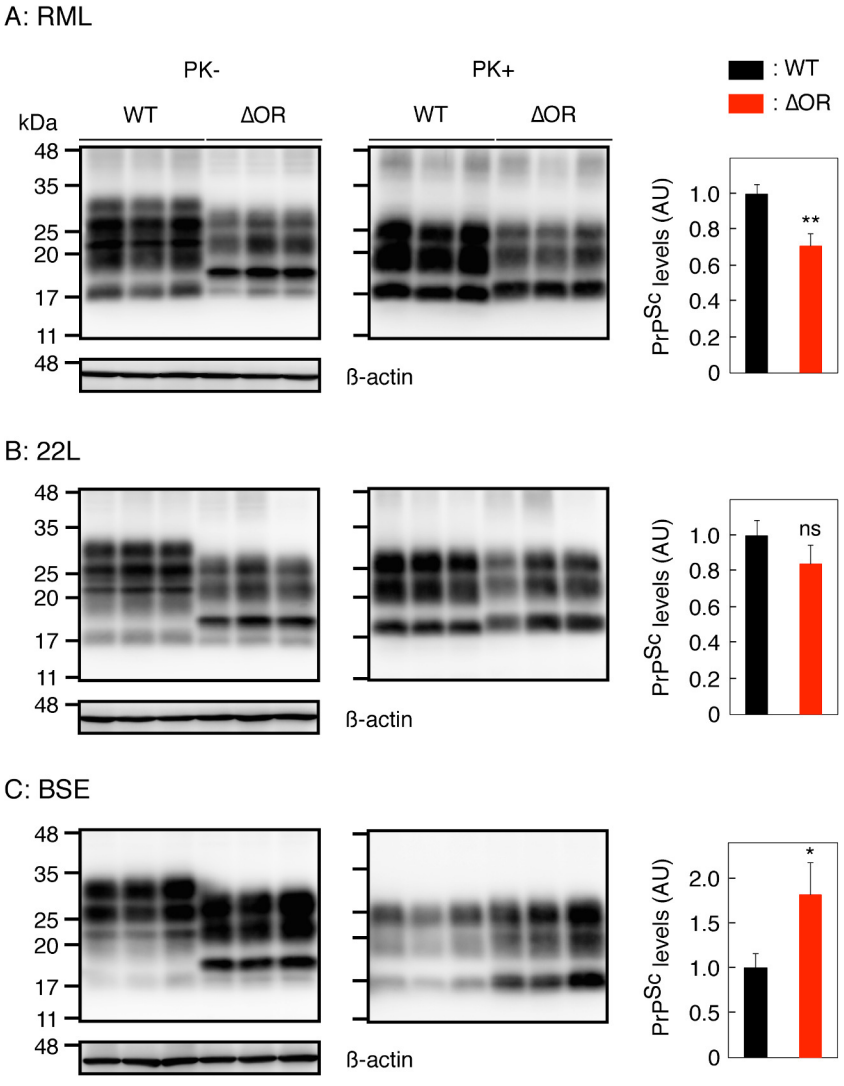
A: RML
PK-
PK+
: WT
: ΔOR
kDa
WT
ΔOR
WT
ΔOR
48
35
25
20
17
11
48
ß-actin
PrPSc levels (AU)
1.0
0.8
0.6
0.4
0.2
0
**
B: 22L
48
35
25
20
17
11
48
ß-actin
PrPSc levels (AU)
1.0
0.8
0.6
0.4
0.2
0
ns
C: BSE
48
35
25
20
17
11
48
ß-actin
PrPSc levels (AU)
2.0
1.5
1.0
0.5
0
*

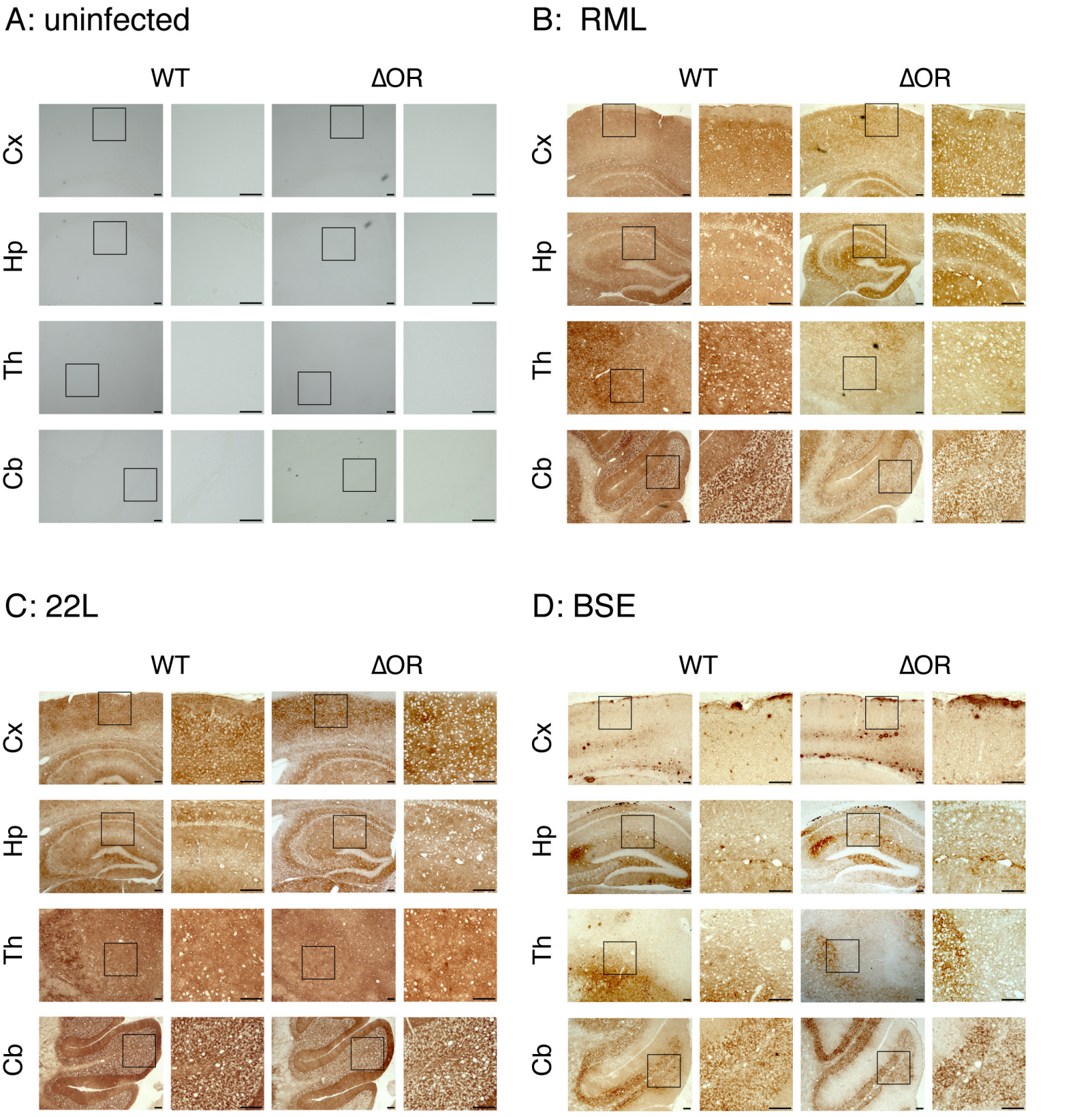
A: uninfected
B: RML
C: 22L
D: BSE
WT
ΔOR
Cx
Hp
Th
Cb

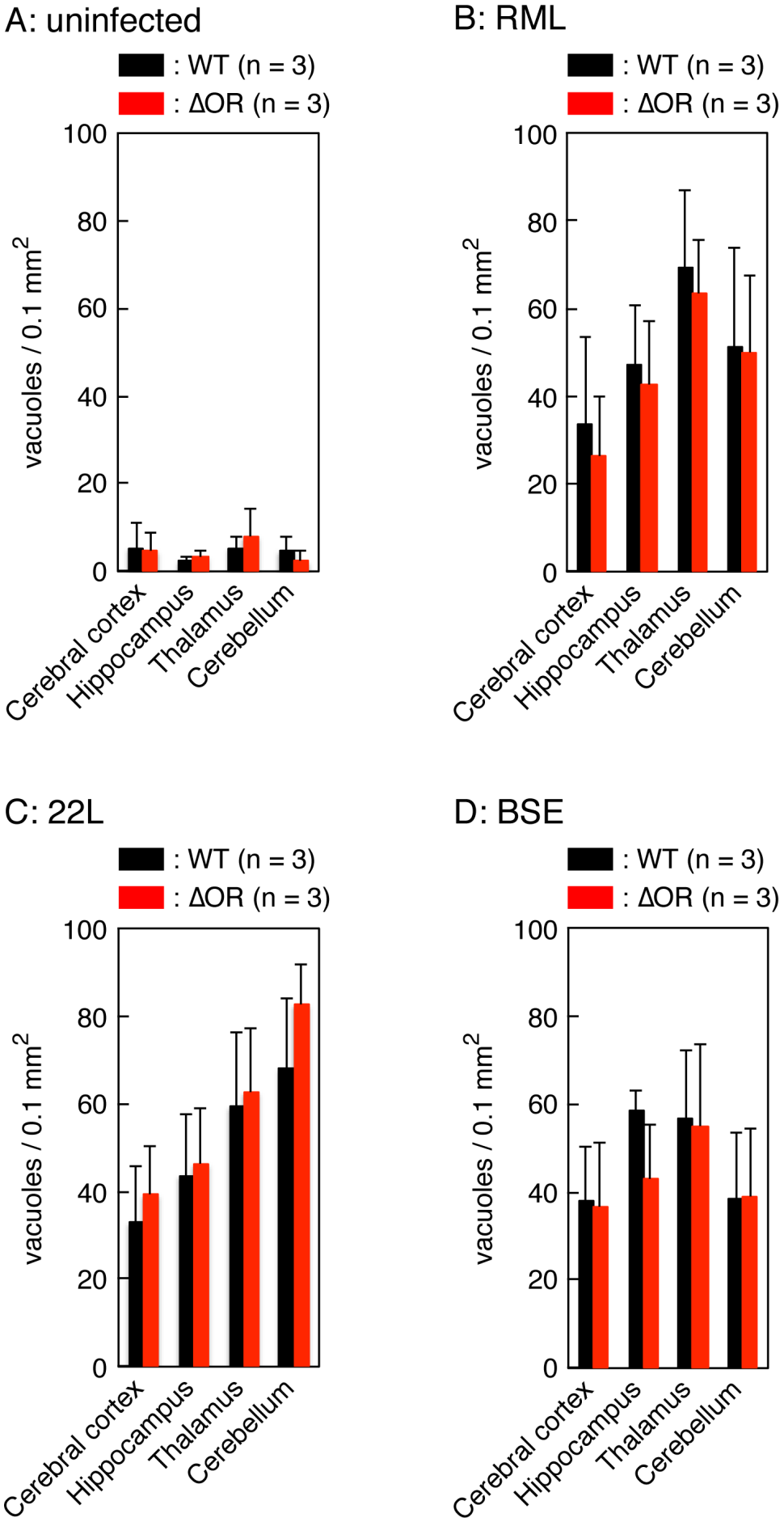
A: uninfected
: WT (n = 3)
: ΔOR (n = 3)
vacuoles / 0.1 mm2
0
20
40
60
80
100
Cerebral cortex
Hippocampus
Thalamus
Cerebellum
B: RML
: WT (n = 3)
: ΔOR (n = 3)
vacuoles / 0.1 mm2
0
20
40
60
80
100
Cerebral cortex
Hippocampus
Thalamus
Cerebellum
C: 22L
: WT (n = 3)
: ΔOR (n = 3)
vacuoles / 0.1 mm2
0
20
40
60
80
100
Cerebral cortex
Hippocampus
Thalamus
Cerebellum
D: BSE
: WT (n = 3)
: ΔOR (n = 3)
vacuoles / 0.1 mm2
0
20
40
60
80
100
Cerebral cortex
Hippocampus
Thalamus
Cerebellum

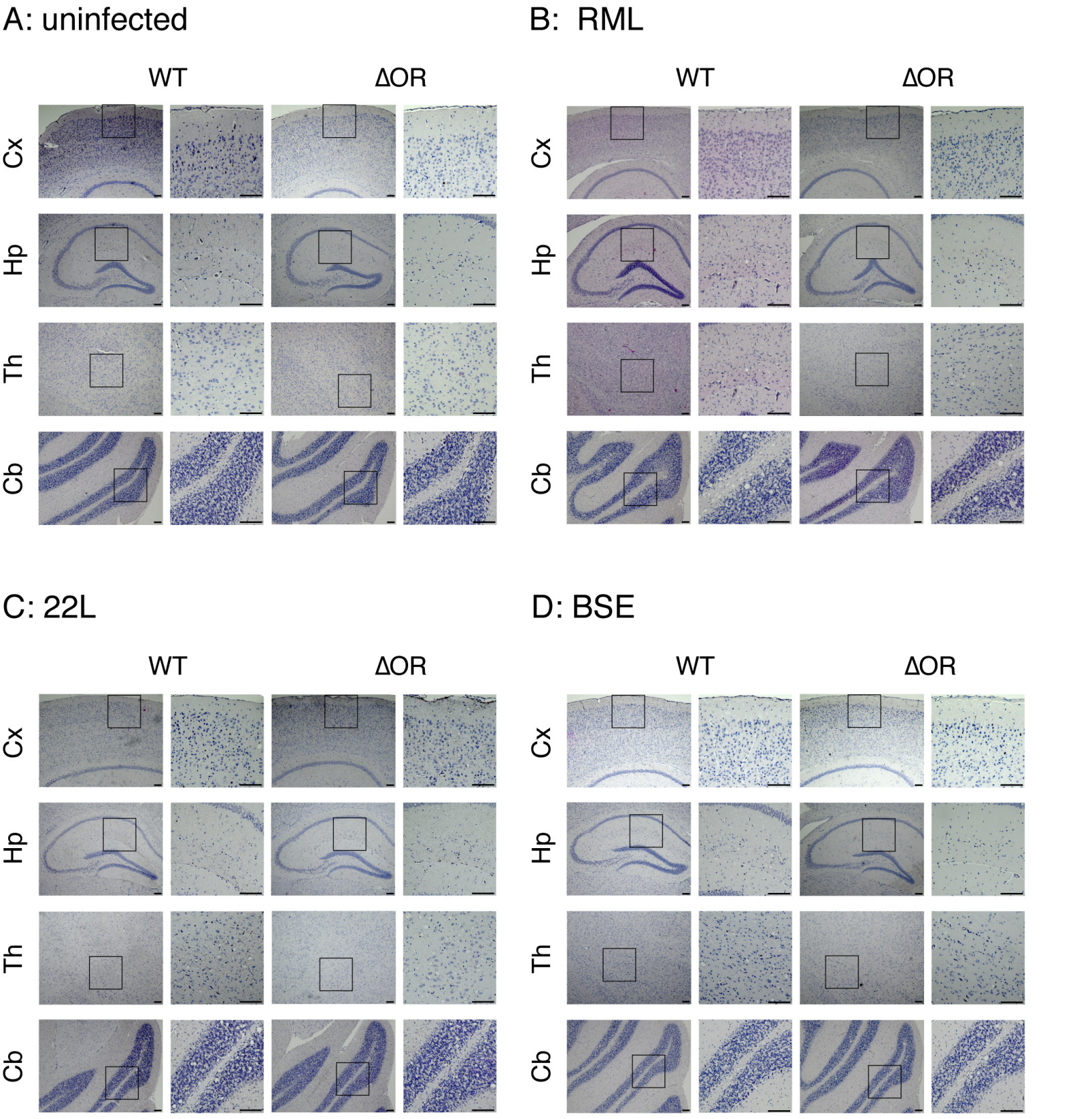
A: uninfected
WT
ΔOR
Cx
Hp
Th
Cb
B: RML
WT
ΔOR
Cx
Hp
Th
Cb
C: 22L
WT
ΔOR
Cx
Hp
Th
Cb
D: BSE
WT
ΔOR
Cx
Hp
Th
Cb

Figure 6

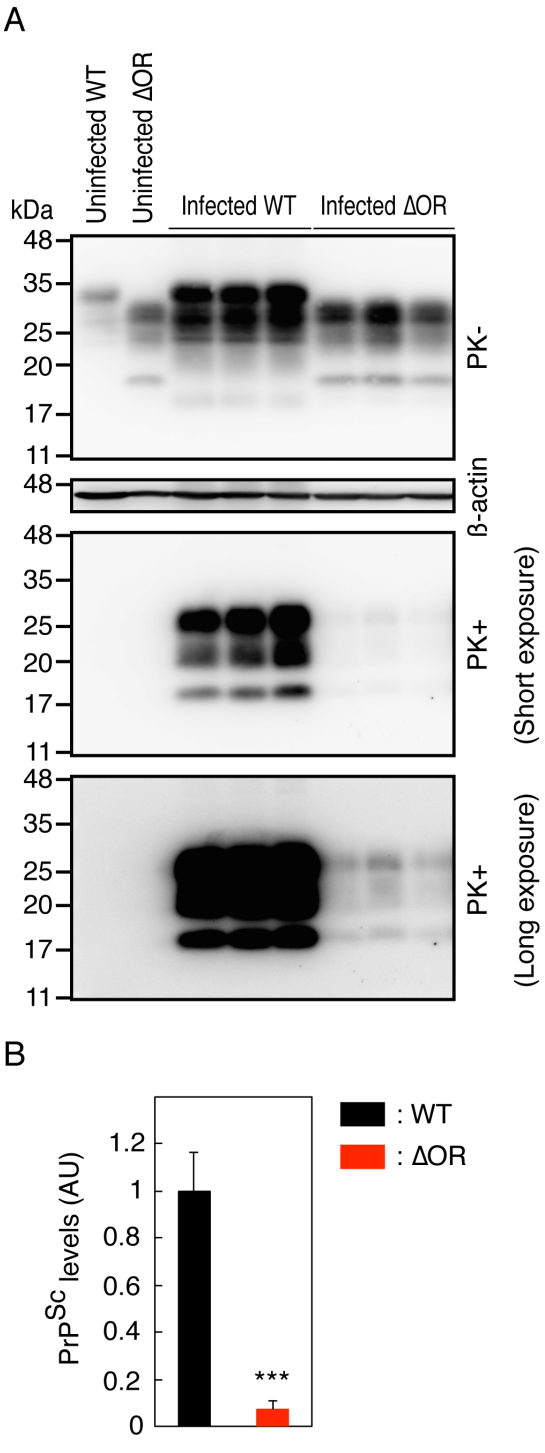
A
Uninfected WT
Uninfected ΔOR
Infected WT
Infected ΔOR
kDa
48
35
25
20
17
11
PK-
β-actin
PK+
(Short exposure)
PK+
(Long exposure)
B
: WT
: ΔOR
PrPSc levels (AU)
1.2
1
0.8
0.6
0.4
0.2
0
***

Figure 7

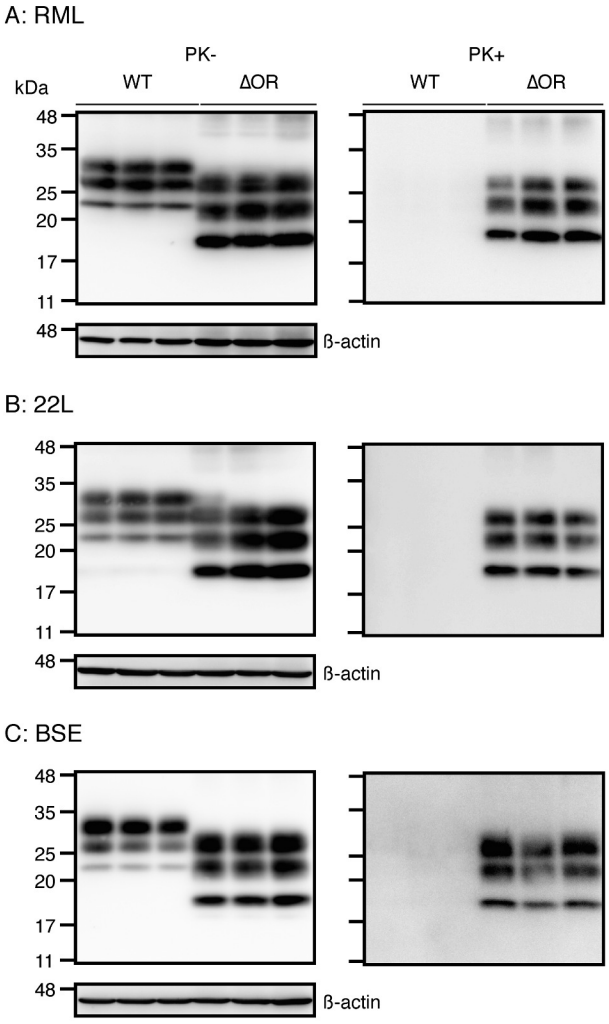
A: RML
PK-
PK+
kDa
WT
ΔOR
WT
ΔOR
48
35
25
20
17
11
48
ß-actin
B: 22L
48
35
25
20
17
11
48
ß-actin
C: BSE
48
35
25
20
17
11
48
ß-actin

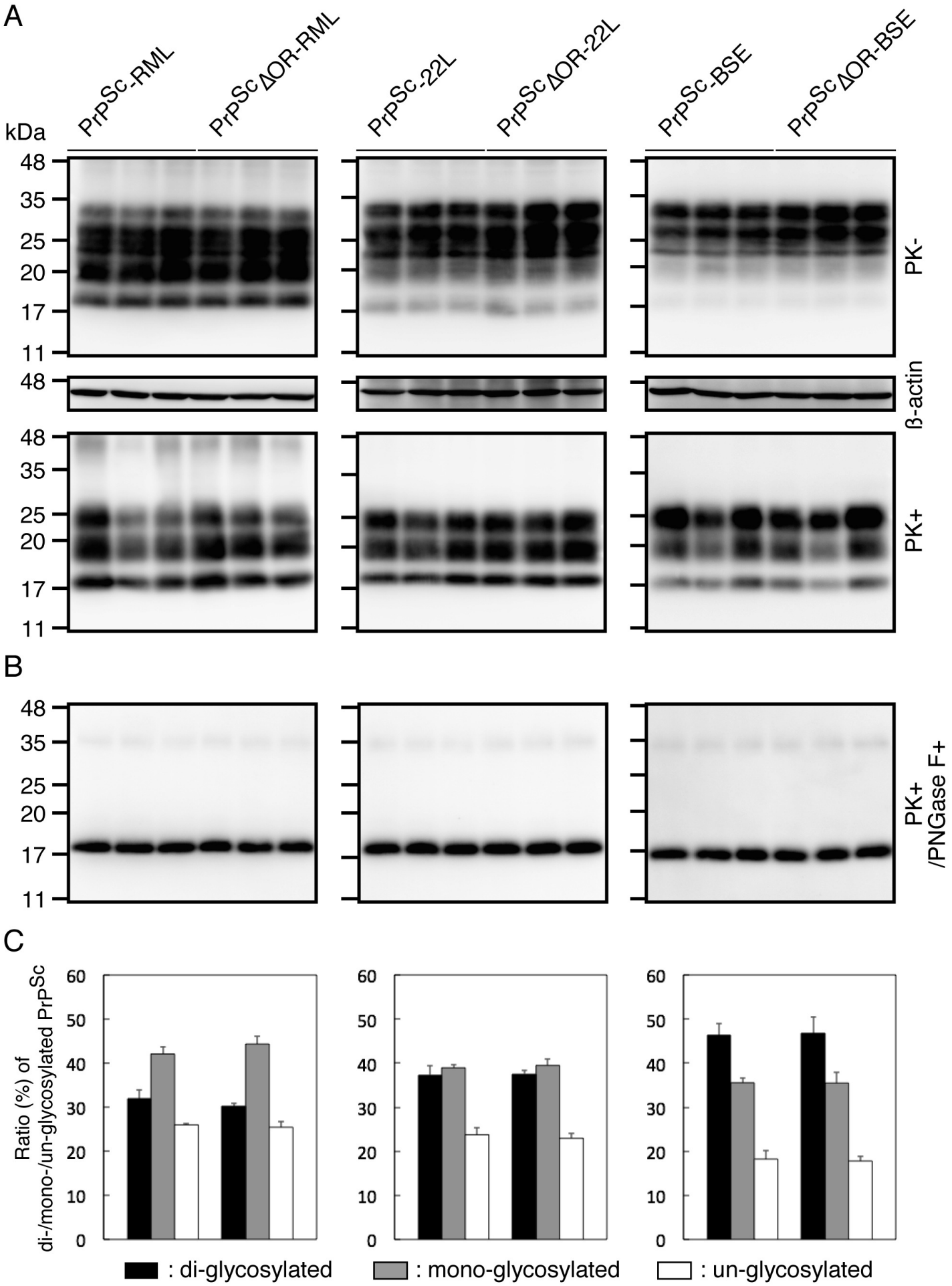
A
PrPSc-RML
PrPScΔOR-RML
PrPSc-22L
PrPScΔOR-22L
PrPSc-BSE
PrPScΔOR-BSE
kDa
48
35
25
20
17
11
PK-
β-actin
PK+
B
PK+
/PNGase F+
C
Ratio (%) of
di-/mono-/un-glycosylated PrPSc
60
50
40
30
20
10
0
: di-glycosylated
: mono-glycosylated
: un-glycosylated